Properties of Primary Motor Cortical Local Field Potentials in the Leg and Trunk Representations During Arm Movements

Adil A. Tobaa[1], Matthew D. Best[2], Karthikeyan Balasubramanian[1], Kazutaka Takahashi[1], and Nicholas G. Hatsopoulos[1,2]

***Abstract*— Large, spatially-distributed populations of motor cortical neurons are recruited during upper limb movements. Here, we examined how beta attenuation, a mesoscopic reflection of unit engagement, varies across a spatially expansive sampling of primary motor cortex in a non-human primate (*macaca mulatta*). We found that electrodes in both the trunk and leg representation of motor cortex exhibit qualitatively similar behavior to electrodes in the arm representation during a planar reaching task, despite the fact that there were no overt movements of the trunk or leg. These findings are interpreted in the context of a state-based brain machine interface.**

I. Introduction

Behavioral neurophysiology studies of the motor cortex typically involve engaging an animal in an upper limb task while simultaneously recording neural activity from the corresponding representation in cortex. However, complementary methodologies such as ECoG and EEG have shown large-scale activation of motor cortex during upper limb movements [1]. These activations are larger than what would be predicted based solely on underlying representation suggesting that motor cortical activation may be more global than behavioral neurophysiologists previously appreciated.

At the same time, it has been demonstrated that spatial variability across the cortical surface may have important implications for brain machine interfaces (BMIs), and that information about movement may be differentially represented across the cortical surface. One recent study demonstrated that movement onset was accompanied by spatio-temporal patterns of attenuation in the beta frequency range (15-30 Hz) of the local field potential (LFP) [2]. This phenomenon of beta attenuation has previously been suggested to act as a switch for minimizing jitter in a BMI, and beta amplitude has shown to be an effective switch for a state-based decoder [3], [4], [5], [6].

In this study, we aimed to further examine properties of beta attenuation prior to movement onset. In particular, we examined beta oscillations in somatotopic regions beyond that of which movement is anticipated to have cortical activity. We characterized electrodes from two chronically implanted microelectrode arrays (128 channels) into leg, trunk, and arm representations in primary motor cortex by observing behavioral effects of intracortical microstimulation (ICMS). We found that in arm movement execution, we observe the beta attenuation phenomenon in arm, leg, and trunk representations. We also found a significant delay in attenuation in leg and trunk relative to arm representations.

*This work was supported by NIH grant R01 NS045853 from the NINDS.

[1]A.A.T., K.B., K.T. and N.G.H. are with the Department of Organismal Biology and Anatomy, University of Chicago, IL 60637, USA (e-mail: {aatobaa, karthikeyanb, kazutaka}@uchicago.edu)

[2]M.D.B. and N.G.H. are with the Committee on Computational Neuroscience, University of Chicago, Chicago, IL 60637, USA (e-mail: {mattbest, nicho}@uchicago.edu)

II. Methods

All surgical and experimental procedures were approved by the University of Chicago Animal Care and Use Committee and conform to the principles outlined in the Guide for the Care and Use of Laboratory Animals (NIH publication no 86-23, revised 1985). One rhesus macaque (*macaca mulatta*) was implanted with two 64-electrode Utah arrays (Blackrock Microsystems, Salt Lake City, UT) in the MI contralateral to its working hand. Electrodes were 1.5 mm in length and arranged in an 8×8 grid with 400 μm inter-electrode spacing. During a recording session, local field potentials (LFPs) from these electrodes were recorded digitally using a Cerebus acquisition system (Blackrock Microsystems, Salt Lake City, UT).

A. Intracortical Microstimulation

We used ICMS to characterize the output effects of each electrode on the two Utah arrays [7]. Cathodal-anodal pulse trains were generated by a Blackrock current stimulator (pulse width: 200 μs, train frequency: 333 Hz, train duration: 75 ms). Current intensities varied between 20 and 50 μA. The specific stimulation protocol that was used to characterize stimulation effects has been described elsewhere (see [8]) and will be briefly summarized here.

Stimulation on each electrode began at 50 μA. If, after several repetitions, no evoked movements were observed, we considered that electrode inactive. However, if evoked movements were observed, we lowered the current intensity until we found the threshold of evoked movements. The movements that were evoked at threshold on an electrode were considered to be its stimulation effects. The sequence of electrodes that we stimulated through was chosen pseudorandomly.

Movements evoked by ICMS were characterized by two experimenters observing the animal. A movement was recorded only if it was visible to both experimenters and readily repeatable. Stimulation was delivered only when the animal appeared to be relaxed.

B. Behavioral task

One male rhesus macaque was operantly conditioned to perform a center-out reaching task. In this task, the animal

978-1-4577-0220-4/16/$31.00 ©2016 IEEE

used a robotic exoskeleton to control the position of a cursor on a screen in front of it. To begin a trial, the animal was required to move the cursor to a center target. The animal was required to hold the cursor within the center target for 600 ms before a peripheral target appeared. Peripheral targets were located at 8 evenly spaced radial intervals around the center target with a distance of 7 cm between the center and peripheral targets. The appearance of the peripheral target served as a GO cue, and the animal could move towards the target. Successful completion of the trial involved moving the cursor to the peripheral target and holding it on the peripheral target for 100 ms. Fluid reinforcement was delivered on every successful trial.

For this study, we defined movement duration as the difference in time between the GO cue and the reward. The slowest 10% of trials were discarded to reduce variability in the neural data arising from behavioral variability.

C. Beta attenuation analysis

We applied preprocessing techniques to estimate beta attenuation from the LFP data [2]. We identified the peak frequency in the beta range (15-30 Hz) and then narrow band filtered the LFPs around that frequency. Visual inspection of 3 electrodes revealed qualitatively different behavior that suggested the electrodes were likely damaged or broken, so they were discarded from subsequent analysis.

We filtered the data with a 4^{th} order Butterworth filter whose peak was at 20 Hz and whose passband was 3 Hz on either side of the peak for a total width of 6 Hz. We applied the Hilbert transform to the band-pass filtered data to compute the instantaneous amplitude of the beta oscillation.

We examined a window of ± 1 second relative to the GO cue for each trial. For each electrode, data were aligned on the GO cue and averaged over trials. We fit a sigmoidal function of the form:

$$f(t) = L + \frac{H - L}{1 + \exp(-r(t - x_0))} \tag{1}$$

using a nonlinear least squares curve fitting routine (Matlab function `nlinfit`) to estimate the amplitude of the trial-averaged beta oscillation, $f(t)$, as a function of time, t, relative to movement onset on each electrode. Here, the constant H indicated the average of the minimum and maximum beta amplitude in a window from -750 to -250 ms before GO cue and corresponded to the maximum asymptote of the sigmoidal curve. The constant L corresponded to the average of the min and max beta amplitude between 250 and 750 ms after the GO cue, and corresponded to the minimum asymptote of the sigmoidal curve. The curve fitting algorithm identified the parameters r and x_0, which were the slope and midpoint of the sigmoidal curve, respectively. The beta attenuation midpoint (BAM) was subsequently used to characterize the timing of attenuation.

Model goodness of fit was assessed using the coefficient of determination, R^2, defined as:

$$R^2 := 1 - \frac{\sum_{t=-750}^{750} (y_t - \hat{y}_t)^2}{\sum_{t=-750}^{750} (y_t - \bar{y})^2} \tag{2}$$

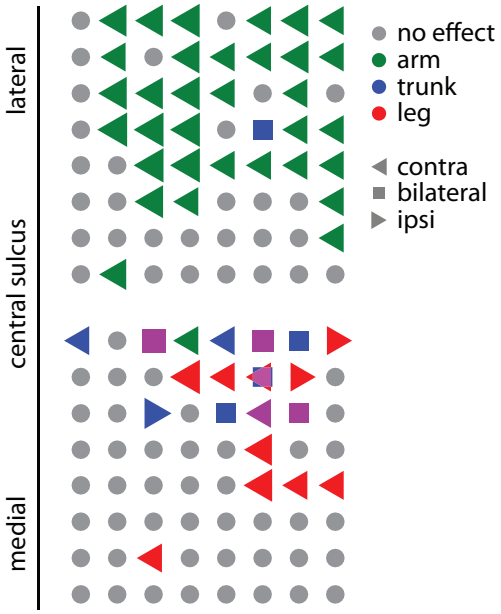

Fig. 1. **Intracortical microstimulation** ICMS was used to characterize the motor outputs of each electrode on two electrode arrays. The two arrays are depicted by two 8×8 grids, arranged spatially along a vertical axis corresponding to actual implanted array locations. Each coordinate represents an electrode for a total of 128 electrodes. Marker color is used to indicate evoked movements by body segment from stimulation (green markers for arm, blue for trunk, red for leg). Evoked movements were observed at 54 electrode sites in total. On 5 electrodes, stimulation evoked both trunk and leg movements (purple markers). Marker shape indicates the laterality of stimulation effects (triangle to the left indicates contralateral, triangle to the right indicates ipsilateral, and square indicates bilateral). The size of each marker is inversely proportional to the threshold current required to evoke movement such that sites with the lowest threshold have the largest markers.

where y_t and $\hat{y}_t$ correspond to the observed and estimated beta amplitude at time t, respectively, and $\bar{y}$ is the average beta amplitude over the interval [-750, 750] ms relative to GO cue.

III. Results

A. ICMS

We used ICMS to characterize the motor output of each electrode on the two electrode arrays. Of the 128 electrodes in our sample, we reliably evoked movements on 54 of them. We further divided the electrodes into groups based on which body segment had evoked movements. We found that arm movements were evoked on 34 electrodes, trunk movements were evoked on 11 electrodes, and leg movements were evoked on 14 electrodes. There were 5 electrodes that evoked both trunk and leg movements. We found that the median current necessary to evoke movement was significantly different across body segments (Kruskal Wallis test, χ^2 with 3 d.o.f. $= 13.96$, $p < 0.003$). Post-hoc testing revealed that the median current necessary to evoke arm movements was significantly lower than the median current needed to evoke trunk movements (Tukey's HSD test, $p < 0.02$).

When stimulation evoked arm movements, the observed stimulation effects were always on the contralateral side of

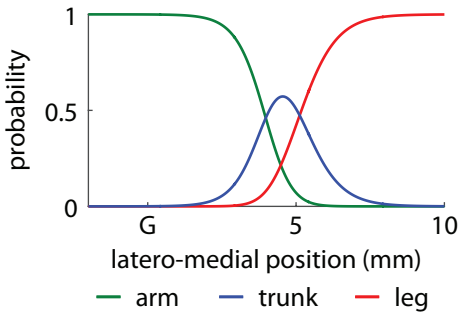

Fig. 2. **Predicting limb representation from electrode location** Position of each electrode along the latero-medial axis of the cortical surface is used as the input to a multinomial logistic regression model. Positions were taken relative to the genu of the arcuate sulcus (indicated with a G on the figure). The model predicted the probability that a given site was associated with arm, trunk, or leg movements. A systematic progression of body representation such that the arm representation was lateral to the trunk representation which was lateral to the leg representation was observed.

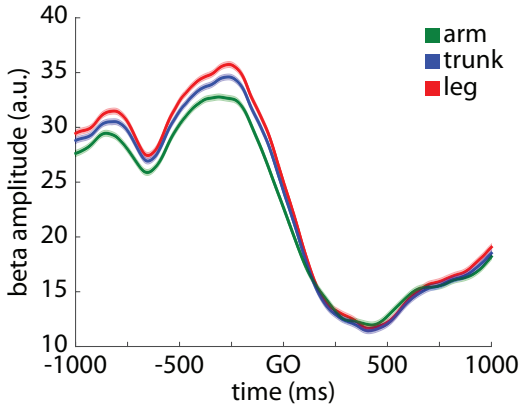

Fig. 3. **The temporal profile of beta activity** Trial-averaged beta amplitude centered on a GO cue for the arm movement task for three different electrodes that evoked arm (green), trunk (blue), or leg (red) muscle twitches when stimulated using ICMS. The beta amplitude attenuates sharply around the GO cue at all three electrodes.

the body from the electrode array. In contrast, electrodes that evoked trunk movements exhibited bilateral stimulation effects roughly half the time (6/11 electrodes), and, in one case, ipsilateral effects. Similarly, electrodes that evoked leg movements exhibited bilateral stimulation effects (3/14 electrodes) or ipsilateral effects (2/14 electrodes) in addition to contralateral effects.

We subsequently considered the spatial distribution of body representation on the cortical surface (Fig. 1). We observed that evoked movements of the trunk and leg were medial to the upper limb representation. We used multinomial logistic regression to quantitatively identify a boundary between different body segments (Fig. 2). We used position along the medio-lateral axis to predict limb representation and observed that the boundary between arm and trunk representation was roughly 4 mm medial to the genu of the arcuate sulcus. Then, approximately 1 mm of cortical surface was devoted to the representation of the trunk. Medial to the trunk representation was the leg representation. Using this approach, we did not attempt to identify the lateral border of the arm representation, or the medial border of the leg representation.

B. Local field potentials

We examined the temporal dynamics of activity in the beta frequency range of the local field potential in the 54 electrodes with stimulation effects. Qualitatively, we observed similar behavior on all electrodes; the amplitude of the beta oscillation attenuated sharply following the GO cue. This attenuation phenomenon was consistent even on electrodes that evoked trunk or leg movements when stimulated (Fig. 3).

We modeled this attenuation phenomenon using a sigmoidal function (Fig. 4). We found that the sigmoidal model well-described the temporal evolution of beta amplitude on all electrodes. Average goodness of fit values were 0.938, 0.945, and 0.947 for arm, leg, and trunk representations, respectively. Across all body segments, the minimum goodness of fit value was 0.892, while the maximum was 0.958.

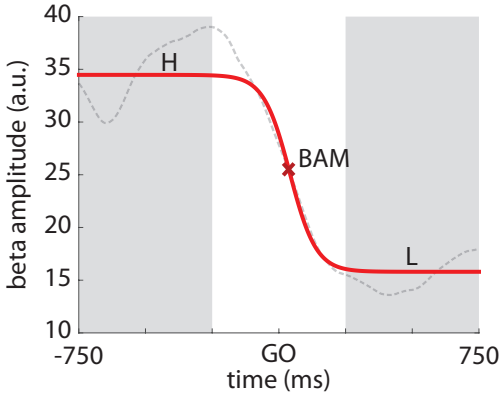

Fig. 4. **Modeling attenuation** The attenuation phenomenon is modeled using a sigmoidal curve. Actual data is shown by grey dotted line. Fitted model is shown in red. The windows of time that were used to find the constant parameters H and L for the sigmoid model are shaded in grey. The beta attenuation midpoint (BAM), used to characterize an instantaneous timing of beta attenuation, is indicated on the figure by a red $\times$.

Having fit sigmoidal models to the beta activity on each electrode, we wanted to compare the timing of beta attenuation across electrodes based on the underlying motor representation revealed by ICMS. We used the midpoint of the sigmoidal curve as our measure of attenuation timing. We found that BAMs were significantly different across body segments (ANOVA, $F_{2,52} = 25.3$, $p < 1e-8$). Post-hoc testing revealed that beta attenuation occurred significantly earlier in the arm representation as compared to the trunk and leg ($p < 1e-5$, Fig. 5).

IV. Discussion

A. ICMS

In this study, we used ICMS to characterize limb representation. Consistent with previous work [9] demonstrating that stimulation effects were weaker at a fixed current intensity, we found that the threshold currents of the trunk and legs were higher than those of the arm. We quantitatively identified the representational boundary between different body

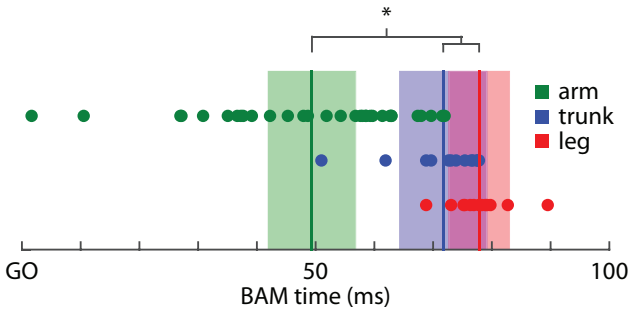

Fig. 5. **The timing of beta attenuation is different across body segments** Here, we show the BAM for every electrode, ordered by the stimulation effects that were observed on each electrode. We found a systematic progression of BAMs such that BAMs occurred earliest on electrodes with arm stimulation effects, then on trunk electrodes and finally on leg electrodes. The average BAM of arm electrodes was significantly closer to the GO cue than for trunk and leg. Shaded areas indicate ± 1 standard error of the mean.

segments on the cortical surface. We observed bilateral and ipsilateral stimulation effects in the trunk and leg representations, but not the upper limb. This finding suggests qualitative differences in the pattern of descending connectivity to the forelimb, trunk, and hindlimb.

B. Beta attenuation

Our results provide further evidence that beta attenuation propagates across the cortical sheet, and is not a simultaneous phenomenon in MI.

Our findings further demonstrate that attenuation is not limited strictly to the body segment that's involved in the task. One possible explanation is that attenuation in other body segments reflects the generation of compensatory movements in other regions of the body. Supporting this interpretation is that beta attenuation occurs later on electrodes that do not evoke arm movements. However, our work is limited in that our experiment consisted of a task utilizing one limb. In future work, we would like to utilize tasks that engage other limbs to determine how closely the beta attenuation timings in different representations correspond with the movements intended by the task.

Further characterizing beta attenuation in this manner would allow us to differentiate limb movements at a mesoscopic scale, based on the orientation of beta.

C. Implications for brain-machine interfaces

While it is perhaps not obvious why arm movements would involve activation of leg and trunk representations in motor cortex, this finding has important implications for brain machine interfaces. If attenuation across cortical representations indicates the timing of compensatory movements, then we may not expect to see similar activation when a subject is controlling a BMI, as no compensation would be required. If activation still occurs, that may be evidence for an underlying connectivity between limbs previously thought independent. In both cases, activity from different body segments could be an important side channel of information for intended behavior. Nevertheless, BMIs may need to consider how leg movements may interfere with the decoding of upper-limb movements.

Furthermore, studies utilizing BMIs may need to account for potential long-term effects of this cross-representational connectivity. If compensatory movements are no longer required while using a BMI, we may find a rearrangement of representational connectivity arising from the plasticity of these neurons.

ACKNOWLEDGMENT

This work made use of computational resources provided by the University of Chicago Research Computing Center.

REFERENCES

[1] C. Neuper, M. Wrtz, and G. Pfurtscheller. ERD/ERS Patterns Reflecting Sensorimotor Activation and Deactivation. In Progress in Brain Research, edited by C. Neuper and W. Klimesch, Volume 159:21122. Event-Related Dynamics of Brain Oscillations. Elsevier, 2006.

[2] M. D. Best, A. J. Suminski, K. Takahashi, K. A. Brown, and N. G. Hatsopoulos. Spatio-Temporal Patterning in Primary Motor Cortex at Movement Onset. Cerebral Cortex, 2016. doi:10.1093/cercor/bhv327.

[3] V. Aggarwal, M. Mollazadeh, A. G. Davidson, M. H. Schieber, and N. V. Thakor. State-Based Decoding of Hand and Finger Kinematics Using Neuronal Ensemble and LFP Activity during Dexterous Reach-to-Grasp Movements. Journal of Neurophysiology 109, no. 12 (June 15, 2013): 306781. doi:10.1152/jn.01038.2011.

[4] A. K. Bansal, W. Truccolo, C. E. Vargas-Irwin, and J. P. Donoghue. Decoding 3D Reach and Grasp from Hybrid Signals in Motor and Premotor Cortices: Spikes, Multiunit Activity, and Local Field Potentials. Journal of Neurophysiology 107, no. 5 (March 1, 2012): 133755. doi:10.1152/jn.00781.2011.

[5] G. Pfurtscheller, and T. Solis-Escalante. Could the Beta Rebound in the EEG Be Suitable to Realize a Brain Switch? Clinical Neurophysiology 120, no. 1 (January 2009): 2429. doi:10.1016/j.clinph.2008.09.027.

[6] C. Kemere, G. Santhanam, B. M. Yu, A. Afshar, S. I. Ryu, T. H. Meng, and K. V. Shenoy. Detecting Neural-State Transitions Using Hidden Markov Models for Motor Cortical Prostheses. Journal of Neurophysiology 100, no. 4 (October 1, 2008): 244152. doi:10.1152/jn.00924.2007.

[7] S. D. Stoney, W. D. Thompson, and H. Asanuma. Excitation of Pyramidal Tract Cells by Intracortical Microstimulation: Effective Extent of Stimulating Current. Journal of Neurophysiology 31, no. 5 (September 1, 1968): 659669.

[8] M. D. Best, A. J. Suminski, K. Takahashi, and N. G. Hatsopoulos. Consideration of the Functional Relationship between Cortex and Motor Periphery Improves Offline Decoding Performance. Annual International Conference of the IEEE Engineering in Medicine and Biology Society. 2014: 486871. doi:10.1109/EMBC.2014.6944714.

[9] H. M. Hudson, D. M. Griffin, A. Belhaj-Saf, and P. D. Cheney. Properties of Primary Motor Cortex Output to Hindlimb Muscles in the Macaque Monkey. Journal of Neurophysiology 113, no. 3 (February 1, 2015): 93749.